THE JOURNAL OF BIOLOGICAL CHEMISTRY

Vol. 277, No. 23, Issue of June 7, pp. 20139–20145, 2002
Printed in U.S.A.

Manipulation of Cholesterol Levels in Rod Disk Membranes by Methyl-β-cyclodextrin

EFFECTS ON RECEPTOR ACTIVATION*

Received for publication, January 18, 2002, and in revised form, February 22, 2002
Published, JBC Papers in Press, March 11, 2002, DOI 10.1074/jbc.M200594200

Shui-Lin Niu, Drake C. Mitchell, and Burton J. Litman‡

From the Section of Fluorescence Studies, Laboratory of Membrane Biochemistry and Biophysics, National Institute on Alcohol Abuse and Alcoholism, National Institutes of Health, Rockville, Maryland 20852

The effect of cholesterol on rod outer segment disk membrane structure and rhodopsin activation was investigated. Disk membranes with varying cholesterol concentrations were prepared using methyl-β-cyclodextrin as a cholesterol donor or acceptor. Cholesterol exchange followed a simple equilibrium partitioning model with a partition coefficient of 5.2 ± 0.8 in favor of the disk membrane. Reduced cholesterol in disk membranes resulted in a higher proportion of photolyzed rhodopsin being converted to the G protein-activating metarhodopsin II (MII) conformation, whereas enrichment of cholesterol reduced the extent of MII formation. Time-resolved fluorescence anisotropy measurements using 1,6-diphenyl-1,3,5-hexatriene showed that increasing cholesterol reduced membrane acyl chain packing free volume as characterized by the parameter f_v. The level of MII formed showed a positive linear correlation with f_v over the range of 4 to 38 mol % cholesterol. In addition, the thermal stability of rhodopsin increased with mol % of cholesterol in disk membranes. No evidence was observed for the direct interaction of cholesterol with rhodopsin in either its agonist- or antagonist-bound form. These results indicate that cholesterol mediates the function of the G protein-coupled receptor, rhodopsin, by influencing membrane lipid properties, *i.e.* reducing acyl chain packing free volume, rather than interacting specifically with rhodopsin.

Cholesterol modulates the function of a variety of membrane proteins including receptors and channels (1–6); this effect can be either inhibitory (1, 3) or stimulatory (2, 5). Currently, two mechanisms are generally discussed regarding the effect of cholesterol on membrane protein function. These are either a specific cholesterol-membrane protein interaction (3–5) or a cholesterol-induced alteration of lipid acyl chain interactions inducing domain or "raft" formation or otherwise affecting bilayer physical properties (3, 4, 7, 8). Discrimination between these two mechanisms requires concomitant characterization of the influence of cholesterol on membrane bilayer structural properties and protein function.

In this study, the visual system, a prototypical G protein-coupled receptor system, is studied to determine the effect of varied cholesterol content in the native ROS[1] disk membrane on receptor activation. In visual transduction, rhodopsin serves as the receptor, and light activates rhodopsin by converting its covalently bound antagonist, 11-*cis* retinal, to its agonist, all-*trans* retinal (9). Within milliseconds of light absorption, MII, the photointermediate that binds and activates the visual G protein transducin, is formed and exists in a metastable equilibrium with its inactive precursor, MI. Previous studies in reconstituted systems clearly demonstrate that the formation of MII is strongly dependent on the physical properties of bilayer lipids (7, 8, 10).

One unique feature of ROS disk membranes is that the cholesterol concentration exists as a gradient running along the long axis of the rod cell (11). The basal disks, which are newly formed, contain 30 mol % cholesterol, whereas the apical disks contain only 5 mol % cholesterol (11). The physiological role of the cholesterol gradient is unclear, although it may be important to visual signal transduction because higher cholesterol is linked to reduced phosphodiesterase activity downstream in the visual cascade (12). The disk membrane is also unusual in that approximately 50% of the phospholipid acyl chains are derived from docosahexanoic acid (DHA), making the disk one of the most polyunsaturated membranes in the human body (13, 14). The major lipid classes in the disk membrane are phosphatidylcholine (PC), phosphatidylenthanolamine, and phosphatidylserine at 40, 41, and 12.5 mol %, respectively (13, 14). The disk also contains low levels of phosphatidylinositol, phosphatidic acid, and diacylglycerol and insignificant amounts of sphingomyelin. The major protein in disk membranes is rhodopsin, which accounts for >90% of the total membrane protein (15, 16). Rhodopsin is the best characterized G protein-coupled receptor in terms of structure and function (17, 18), which makes the disk membrane an ideal system for investigating the mechanism whereby cholesterol modulates receptor function.

In this study, disk membranes varying in cholesterol concentration were prepared using methyl-β-cyclodextrin (MBCD) as a cholesterol donor or acceptor. The influence of cholesterol on rhodopsin activation was characterized by examining the conformational equilibrium between MI and MII. The effect of cholesterol on membrane acyl chain packing was characterized using the time-resolved decay of the fluorescence anisotropy of DPH (19, 20). Examining the cholesterol dependence of the absorption spectrum of the dark-adapted and light-activated

* The costs of publication of this article were defrayed in part by the payment of page charges. This article must therefore be hereby marked "*advertisement*" in accordance with 18 U.S.C. Section 1734 solely to indicate this fact.

‡ To whom correspondence should be addressed: 12420 Parklawn Dr., Rm. 158, Rockville, MD 20852. Tel.: 301-594-3608; Fax: 301-594-0035; E-mail: litman@helix.nih.gov.

[1] The abbreviations used are: ROS, rod outer segment; DHA, docosahexanoic acid; DPH, 1,6-diphenyl-1,3,5-hexatriene; DSC, differential scanning calorimetry; f_v, phospholipid acyl chain packing free volume; MBCD, methyl-β-cyclodextrin; MI, metarhodopsin I; MII, metarhodopsin II; K_{eq}, MI-MII equilibrium constant; PC, phosphatidylcholine; TBS, Tris-buffered saline; PIPES, 1,4-piperazinediethanesulfonic acid.

states of rhodopsin allowed an assessment of any cholesterol-induced structural perturbation in the intrahelical binding pocket of the retinal chromophore. Perturbation of the overall structural stability of rhodopsin by cholesterol was assessed using DSC to measure the thermal denaturation of rhodopsin. Our results demonstrate that cholesterol inhibits rhodopsin activation by reducing the equilibrium concentration of MII in the absence of direct interaction with rhodopsin; however, this effect is linked directly to cholesterol-induced reductions in membrane acyl chain packing free volume. These results indicate that cholesterol modulates rhodopsin activation by influencing membrane phospholipid acyl chain packing rather than via direct interaction with rhodopsin.

EXPERIMENTAL PROCEDURES

Sample Preparation—Cholesterol and MBCD were purchased from Sigma. Cholesterol-MBCD complex was prepared by premixing cholesterol and MBCD as solids (weight ratio of 1:20) followed by solubilization in degassed TBS buffer consisting of 10 mM Tris, 60 mM NaCl, 30 mM KCl, 50 μM diethylenetriamine pentaacetic acid, pH 7.5. The solution was sealed in argon and shaken at room temperature overnight. The final solution was filtered through a 0.45-μm filter and assayed for final cholesterol concentration (21). Cholesterol CII assay kit was from WAKO (Richmond, VA). BCA protein assay kit and Coomassie Plus protein assay kit were from Pierce. ROS were isolated from frozen bovine retinas (James and Wanda Lawson, Lincoln, NE) as described by Miller *et al.* (22). Intact disk membranes were prepared using the Ficoll floatation method (15). Unless otherwise stated, all disk manipulations and measurements were conducted under argon in the dark with the aid of night vision goggles.

Membrane Cholesterol Manipulation Using MBCD—Cholesterol-depleted disk membranes were prepared by incubating disk membranes with various concentrations of MBCD (0–40 mM) in TBS buffer, pH 7.5. Samples were incubated at room temperature in the dark for 2 h on a shaker. Measurements of disk cholesterol content at several time points indicated that 2 h was a sufficient incubation time to reach equilibrium for cholesterol exchange between disk membranes and MBCD (data not shown). The MBCD-treated disk membranes were then separated from MBCD by centrifugation followed by two additional washes in TBS buffer. The membrane pellet and MBCD-containing supernatant were assayed for cholesterol (21), phospholipids (23), and rhodopsin (24, 25), and the mole percentage of cholesterol to total phospholipids in disk membranes was determined. Cholesterol-enriched disk membranes were prepared similarly, except that disk membranes were incubated with cholesterol-loaded MBCD (0–1.2 mM cholesterol in 10 mM MBCD). The mole percentage of cholesterol in samples prepared in this study were used as follows: 4, 12, 15, and 38 mol %, where the 15 mol % cholesterol sample was the native disk membrane without MBCD treatment.

MI-MII Equilibrium Measurements—Disk membranes were extruded through 0.2-μm membranes using a LiposoFast extruder (Avestin, Ottawa, Canada) to reduce light scattering. The final sample was suspended at 0.3 mg/ml in pH 7.5 TBS buffer for UV-visible absorption measurements. Briefly, 110-μl samples were equilibrated in a quartz cuvette for 5 min at 37 °C in the dark. Four spectra of each sample were recorded at the following time points: 1) after temperature equilibration in the dark; 2) 3 s after the sample was partially bleached (20–30%) by a flash lamp equipped with a 520-nm broad bandpass filter; 3) after incubation with 30 mM hydroxylamine for 10 min; 4) after the sample was fully bleached. The first absorption spectrum is of dark-adapted rhodopsin. Within milliseconds, photoexcited rhodopsin exists in a metastable equilibrium between MI and MII. The equilibrium spectra of MI and MII and associated K_{eq} were determined by taking appropriate difference spectra as previously described (26).

Fluorescence Measurements—Samples for fluorescence measurements were made immediately prior to use by diluting a concentrated disk solution to 100 μM phospholipid and adding 0.3 μl of DPH in tetrahydrofuran to yield a final phospholipid/DPH ratio of 300:1. Argon was streamed into the cuvette during this entire process, and the added tetrahydrofuran was allowed to evaporate by continuing the argon stream for several minutes following addition of DPH. All samples were incubated at 40 °C in darkness for 1 h before being brought to 37 °C for measurement. Total optical density (scatter plus absorption) at the wavelength of fluorescence excitation was less than 0.1. Fluorescence lifetime and differential polarization measurements were performed with a K2 multifrequency cross-correlation phase fluorimeter (ISS, Urbana, IL). Excitation at 351 nm was provided by an Innova 307 argon ion laser (Coherent Radiation, Palo Alto, CA). Lifetime and differential polarization data were acquired at 15 modulation frequencies, logarithmically spaced from 5 to 200 MHz using decay acquisition software from ISS as previously described (20). Both total intensity decay and differential polarization measurements were repeated with each cholesterol composition a minimum of three times.

Total fluorescence intensity decays were modeled as the sum of two discrete exponential decays. To compare the effects of cholesterol content on the average fluorescence lifetime, the intensity-weighted average fluorescence lifetime $\langle\tau\rangle$ was calculated. Measured polarization-dependent differential phases and modulation ratios for each sample were combined with the measured total intensity decay to yield the anisotropy decay, $r(t)$. An empirical description of all anisotropy decays was obtained via analysis in terms of a simple sum of exponentials of the form shown in Equation 1,

$$r(t)=(r_o-r)(\beta_1\exp(-t/\phi_1)+\beta_2\exp(-t/\phi_2))+r \qquad \text{(Eq. 1)}$$

where r_o is the fluorescence anisotropy at $t = 0$, r_∞ is the non-decaying anisotropy remaining at the longest time measured in the experiment, ϕ_1 is the rotational correlation time, and β_1 is the functional contribution of each exponential term.

The empirical sum of exponentials model provides information about fluorophore rotational correlation times and the extent to which the fluorescence anisotropy can decay to zero. However, it provides no information regarding the range of equilibrium angular orientations to which DPH is restricted by the surrounding matrix of phospholipid acyl chains. Therefore all data were also analyzed using the Brownian rotational diffusion model as previously described (20). It is useful to calculate a single parameter that corresponds to the extent to which the equilibrium orientational freedom of DPH is restricted by the phospholipid acyl chains. Such a parameter is f_∞, which is directly proportional to the extent to which DPH is randomly oriented in the membrane (19, 27). All analyses of differential polarization data were performed with NONLIN (10, 28), and subroutines specifying the fitting function were written by the authors.

DSC Measurements—DSC measurements were performed in a Nanoscan II calorimeter (Calorimetry Sciences, Provo, UT). Disk membranes at a concentration of 1.0 mg/ml rhodopsin in pH 7.0 PIPES basic salt (PIBS) buffer containing 10 mM PIPES, 60 mM KCl, 30 mM NaCl, and 50 μM diethylenetriamine pentaacetic acid were degassed and loaded into sample cells in complete darkness. The cell was sealed under a stream of argon and pressurized to 2.8 atm. After temperature equilibration was reached, samples were scanned at 0.5 °C/min, and the data were analyzed using Cp-Cal 2.1 provided by Calorimetry Sciences.

RESULTS

Manipulation of the Disk Membrane Cholesterol Content by MBCD—The native ROS disk membrane preparation contained 15 mol % cholesterol. Incubation of disk membranes with increasing amounts of MBCD resulted in a successive depletion of cholesterol from disk membranes (Fig. 1*A*). In the presence of 10 mM MBCD mixed with 1 mM disk membrane phospholipids, 65% of cholesterol was removed from disk membranes. Higher concentration of MBCD resulted in a further depletion of cholesterol from disk membranes. Control experiments were conducted to evaluate the potential risks for co-removal of phospholipids and rhodopsin from disk membranes by MBCD. No rhodopsin was extracted from disk membranes in the presence of MBCD up to 40 mM, indicating that MBCD has no affinity for rhodopsin relative to disk membranes. However, a small fraction of phospholipids was extracted from disk membranes at lower MBCD concentrations (Table I). The amount of phospholipids extracted became significant at concentrations of MBCD above 15 mM. We used 10 mM MBCD in all cholesterol depletion preparations to maximize the removal of cholesterol while minimizing the extraction of phospholipids.

Analysis of the data in Fig. 1*A* (according to a simple equilibrium partitioning model) resulted in a partition coefficient of 5.2 ± 0.8, indicating that under conditions of equal amounts of disk membrane and MBCD, cholesterol partitions 5.2-fold higher into disk membranes than into MBCD. The equilibrium partition model was tested by enriching the amount of choles-

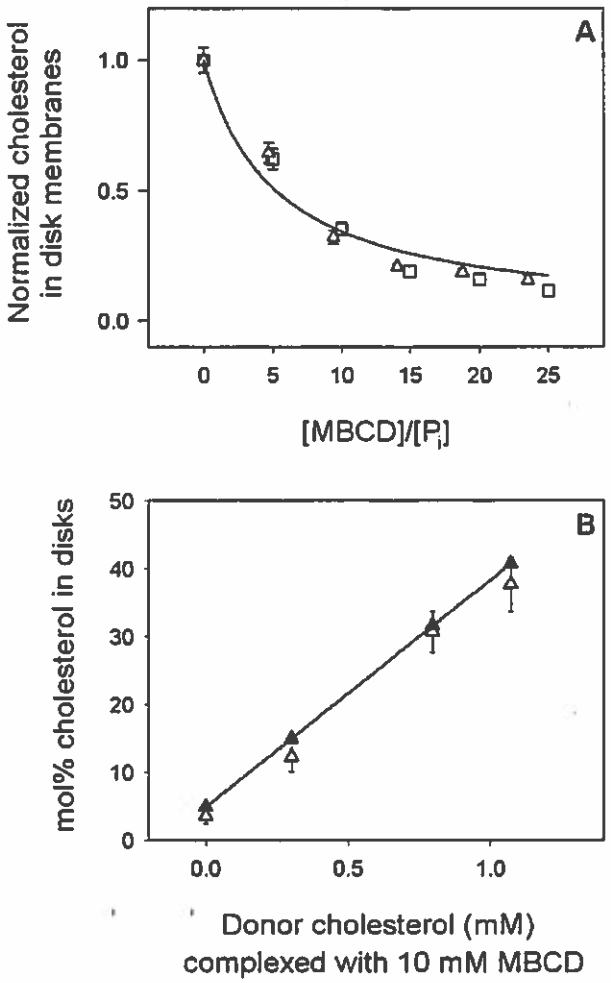

FIG. 1. **Manipulation of disk cholesterol levels.** *A*, disk cholesterol depletion by MBCD. Cholesterol in MBCD-treated disks, normalized to that in control disks without MBCD treatment, is plotted against the molar ratio of MBCD to total phospholipids, [MBCD]/[P_i], in the disk membranes. Data shown are from two sets of experiments with 1.0 mM (□) and 1.6 mM (△) disk membrane phospholipids. The *solid curve* was fitted according to equilibrium partitioning of cholesterol between MBCD and disk membranes. *B*, cholesterol enrichment in 1.0 mM disk membrane phospholipids by cholesterol-MBCD complex. △, experimentally determined cholesterol concentration in disk membranes; ▲, calculated cholesterol concentration in disk membranes according to the equilibrium partition model using a partition coefficient derived from the data in *A*.

TABLE I
Amount of phospholipids extracted from disk membranes by MBCD

[MBCD]	phospholipids extracted from disk membranes by MBCD
mM	%[a]
0	0.0 (± 0.2)
5	0.8 (± 0.1)
10	1.4 (± 0.1)
15	1.8 (± 0.1)
20	4.3 (± 0.3)
25	8.0 (± 0.7)
30	8.6 (± 0.5)

[a] The number in parentheses is ± S.D.

terol in disk membranes by incubating them with 10 mM MBCD preloaded with various amounts of cholesterol. The agreement between observed levels of cholesterol enrichment and the levels calculated from the equilibrium partition model as shown in Fig. 1*B* confirm that an equilibrium-partition model is followed for cholesterol exchange between MBCD and

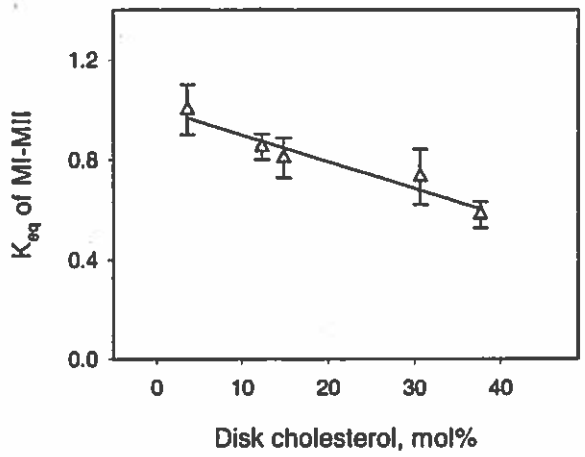

FIG. 2. **Effect of cholesterol on the MI-MII equilibrium constant (K_{eq}).** Equilibrium spectra were acquired in disk membranes containing 4, 12, 15, and 38 mol % cholesterol in pH 7.5 TBS buffer at 37 °C. Sample containing 15 mol % cholesterol was the control disks without MBCD treatment, whereas other samples were prepared using MBCD as cholesterol donor or acceptor. K_{eq} was calculated from deconvolved MI-MII equilibrium spectra as described under "Experimental Procedures."

disk membranes. Using the combination of MBCD and cholesterol-MBCD complex, we were able to manipulate the cholesterol concentration in disk membranes in a wide range.

Cholesterol Inhibits Rhodopsin Activation—The effect of membrane cholesterol on rhodopsin activation was investigated in disk membranes by varying the membrane cholesterol concentration. Overall, an inverse correlation between membrane cholesterol content and K_{eq} for the MI-MII equilibrium was observed at 37 °C, as shown in Fig. 2. In control disk membranes the cholesterol concentration was 15 mol %, and K_{eq} was 0.81 ± 0.08. In cholesterol-depleted disk membranes, which have a cholesterol level of 4 mol %, similar to the 5 mol % found in disks in the apical portion of the ROS, K_{eq} was 1.00 ± 0.10. In disk membranes containing 31 mol % cholesterol, which correspond to cholesterol levels of the basal disks in the ROS, K_{eq} was reduced to 0.73 ± 0.11. At physiological temperature, the cholesterol gradient in ROS, which spans from 5 to 30 mol %, corresponds to a shift in Gibbs free energy (ΔG) associated with MI-MII equilibrium toward a more positive value by 189 cal/mol, resulting in the formation of approximately 17% less MII.

Cholesterol Reduces Membrane Free Volume (f_v)—Variation in cholesterol content of disk membranes resulted in substantial changes in the motional and orientational properties of the hydrophobic fluorescence probe DPH as well as the DPH fluorescence lifetime. The intensity-weighted average fluorescence lifetime of DPH varied directly with membrane cholesterol content and ranged from $<\tau>$ of 7.7 ± 0.1 ns for 4 mol % cholesterol to $<\tau>$ of 9.8 ± 0.1 ns for 38 mol % cholesterol at 37 °C (Fig. 3*A*). The magnitude of the increase in DPH fluorescence lifetime with increased cholesterol is very similar to what is observed in pure lipid bilayers (20), and it reflects cholesterol-induced reduction in water penetration. Alteration in the rate of DPH motion with changes in membrane cholesterol content is indicated by changes in $D_\perp$, the diffusion constant for DPH rotation about its long axis (obtained from the Brownian rotational diffusion model). Depletion of cholesterol increased $D_\perp$, indicating more rapid rotational motion of DPH, whereas cholesterol enrichment reduced $D_\perp$ as shown in Fig. 3*B*. A series of studies demonstrate that the overall orientational order of DPH in a phospholipid bilayer is well summarized by the parameter f_v, a measure of phospholipid acyl chain packing

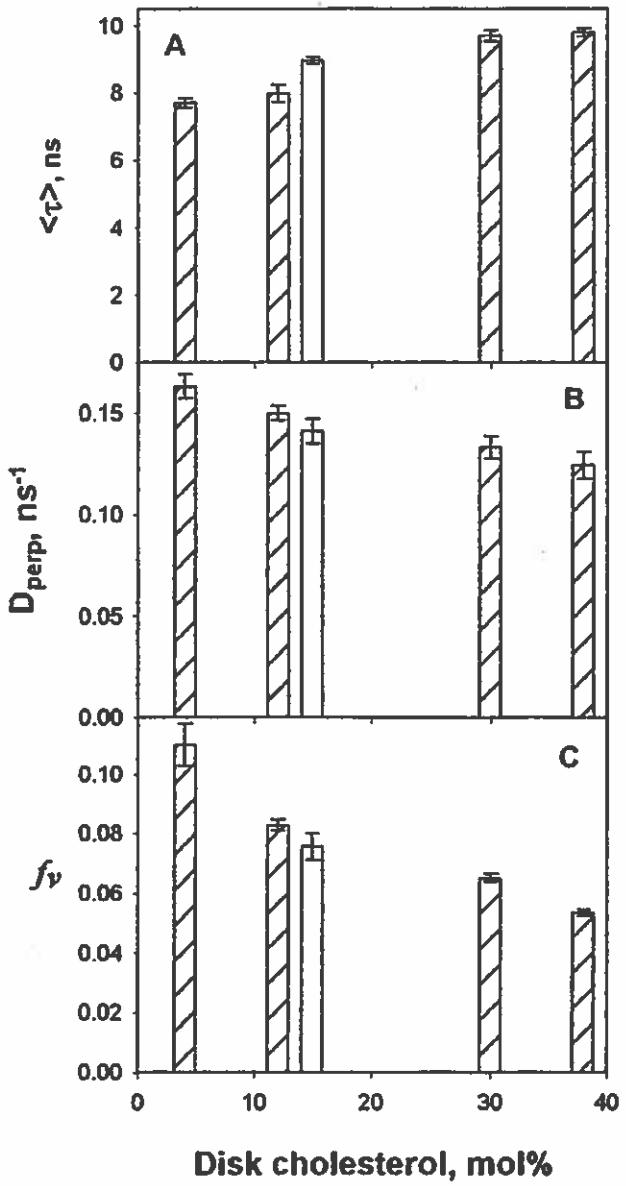

FIG. 3. **Summary of the effects of cholesterol concentration in the disk membrane on DPH fluorescent lifetime and anisotropy decay.** *A*, intensity-weighted average fluorescence lifetime, $<\tau>$. *B*, the diffusion coefficient for DPH rotation about its long axis. *C*, phospholipid acyl chain packing free volume parameter, f_v. This parameter is calculated from the DPH orientational distribution function that results from analysis of anisotropy decay data in terms of the Brownian rotational diffusion model (20). Samples contained the same cholesterol levels as described in the legend to Fig. 2. *Open bars* at 15 mol % cholesterol represent the control disk sample, which received no MBCD treatment.

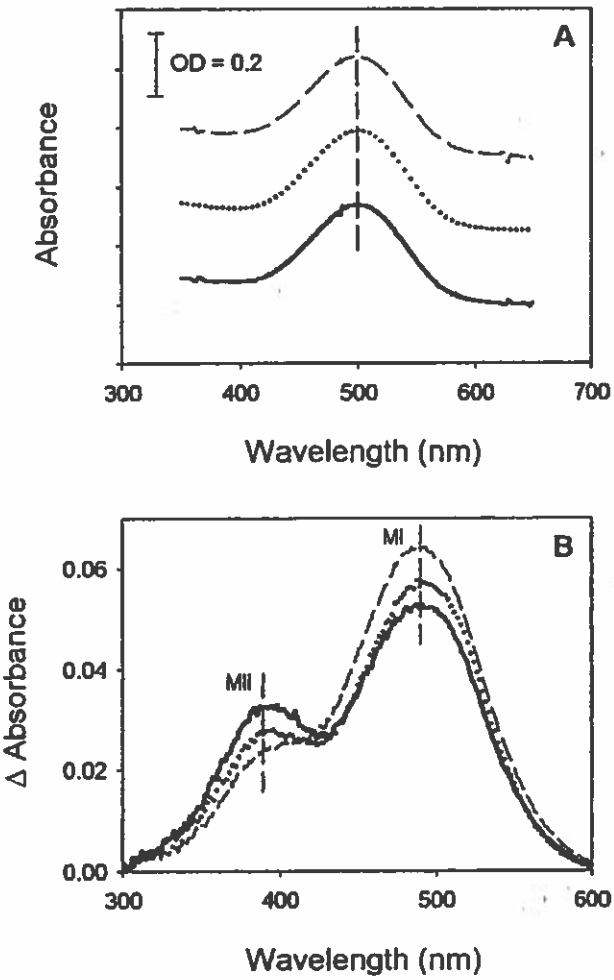

FIG. 4. **Effect of cholesterol on rhodopsin absorption spectrum.** UV-visible absorption spectra of dark-adapted rhodopsin (*A*) and light-activated rhodopsin (*B*) from cholesterol-depleted disks containing 5 mol % cholesterol (*solid curves*), control disks containing 15 mol % cholesterol (*dotted curves*), and cholesterol-enriched disks containing 47 mol % cholesterol (*dashed curves*). All spectra were acquired in TBS, pH 7.5, at 20 °C. Absorption peaks for dark-adapted rhodopsin, MI, and MII are marked with *dashed lines* for comparison.

free volume (19, 20). The untreated disk membranes had a cholesterol content of 15 mol %. At 37 °C upon reduction of membrane cholesterol to 4 mol %, f_v increased by 45%, whereas enrichment of cholesterol to 38 mol % reduced f_v by 30% as shown in Fig. 3*C*. Intermediate cholesterol contents had varied f_v values within this range. Previous studies show that this reduction in f_v corresponds to a significant decrease in acyl chain packing free volume comparable with the change in acyl chain packing induced by a reduction in temperature of 10 °C.

Direct Rhodopsin-Cholesterol Interaction?—The absorption spectrum of the retinal chromophore in rhodopsin is determined by its interactions with the amino acid side chains of opsin and is therefore sensitive to protein conformational changes in the intrahelical retinal-binding site (29, 30). Changes in any rhodopsin absorption spectrum in disks with variation in cholesterol content would reveal the structural perturbation in the intrahelical domain of rhodopsin induced by cholesterol. Depletion or enrichment of cholesterol in disk membranes had no effect on the absorption spectrum of dark-adapted rhodopsin, which has an absorption maximum at 498 nm (Fig. 4*A*). The absorption spectrum of photoactivated rhodopsin is established within tens of milliseconds and consists of two absorbing species, MI (490 nm) and MII (388 nm), which exist in a metastable equilibrium. The absorption peaks of both MI and MII were unchanged by cholesterol depletion or enrichment in disk membranes (Fig. 4*B*). However, relative intensities of the MI and MII absorption bands were shifted by cholesterol manipulation, reflecting the modulation of K_{eq} by cholesterol. Because cholesterol enrichment or depletion induced no shift in the absorption peak position of either dark-adapted or light-activated rhodopsin, specific interaction between cholesterol and rhodopsin could be ruled out.

Effect of Cholesterol on Rhodopsin Thermal Stability—The thermal unfolding of rhodopsin in ROS disk membranes was

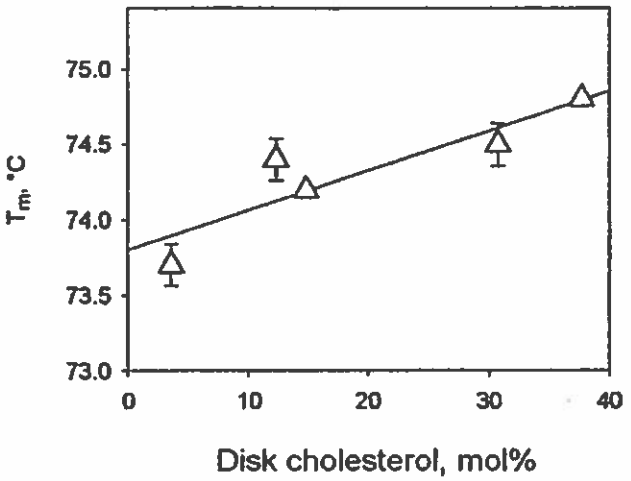

FIG. 5. **Effect of membrane cholesterol concentration on the thermal denaturation of rhodopsin.** Samples contained 1.0 mg/ml rhodopsin in pH 7.0 PIBS buffer and were scanned at 0.5 °C/min.

examined via DSC. Overall, increased cholesterol levels in disk membranes resulted in a higher transition temperature for the thermal denaturation of rhodopsin. In control disk membranes that had not been exposed to MBCD rhodopsin underwent thermal unfolding at 74.2 ± 0.05 °C, in close agreement with previous investigations (31). Addition of cholesterol to 38 mol % raised the thermal unfolding temperature of rhodopsin to 74.8 °C, and depletion of cholesterol to 4 mol % lowered the thermal unfolding temperature to 73.7 °C as shown in Fig. 5.

DISCUSSION

Membrane Cholesterol Manipulation Using MBCD—Our results demonstrate that disk membranes can be depleted or enriched with cholesterol using MBCD as a cholesterol donor or acceptor. This method has advantages of shorter preparation time, wider ranges of cholesterol concentrations achieved in disk membranes, and more quantitative data when compared with the previous method of manipulating the cholesterol content of disk membranes using phospholipid vesicles (32). Cholesterol exchange between disk membranes and MBCD was found to follow an equilibrium-partition model with a partition coefficient of 5.2 in favor of the disk membrane. The same model may also apply to other cellular membranes in which MBCD is used to manipulate membrane cholesterol. However, MBCD should be used with caution because it was found to bind phospholipids as well, especially at concentrations of MBCD greater than 15 mM (Table I). If significant amounts of phospholipid are extracted from membranes by MBCD, membrane structure may be disturbed unintentionally. Thus, effects caused by a loss of phospholipid may inadvertently be attributed to changes in cholesterol concentration. A general guideline for preparation of cholesterol-depleted membranes is to use a high molar ratio of MBCD/membrane phospholipid (up to 10:1) to maximize the transfer of cholesterol from membranes to MBCD. For preparation of cholesterol-enriched membranes a low ratio of MBCD/membrane phospholipid and a high donor cholesterol concentration should be used to maximize transfer of cholesterol from MBCD to membranes.

Cholesterol Inhibits Rhodopsin Activation—Elevated cholesterol levels in disk membranes correlated with lower values of K_{eq} for the MI-MII equilibrium, which is consistent with studies in reconstituted rhodopsin-containing model membranes (33). The highest K_{eq} values were observed in disk membranes containing the lowest amount of cholesterol (4 mol %), which infers a physiological consequence of the cholesterol gradient along the stack of disks in ROS (11). The basal disks contain the highest amount of cholesterol (30 mol %), which should have lower K_{eq} values. These disks are gradually depleted of cholesterol as they move to the top of the stack. The apical disks contain only 5 mol % cholesterol so that increased rhodopsin activation is achieved. Because visual signaling is transferred from rhodopsin to phosphodiesterase via coupling to transducin, the cholesterol effect on rhodopsin activation would likely be propagated along the signaling cascade. This is consistent with a study by Boesze-Battaglia and Albert (12) in which a lower phosphodiesterase activity was observed in disks with higher cholesterol levels.

Mechanism of Receptor Inhibition by Cholesterol—Cholesterol alters the function of a variety of receptors and channels (1–5). The current mechanistic views on cholesterol-induced effects on membrane protein function fall into the following two categories: 1) modulation by specific cholesterol-protein interaction and 2) modulation via cholesterol-induced changes in phospholipid acyl chain packing. To date most studies have focused on changes in protein function upon cholesterol removal and/or enrichment (1–6). Perturbations of protein structure or membrane physical properties by cholesterol have been largely unexamined in native membranes under physiological conditions. A remaining challenge for those systems reported to involve specific interactions with cholesterol is to characterize the nature of such interaction sites.

In this study the variation in acyl chain packing in native disk membranes induced by cholesterol was examined using the time-resolved decay of fluorescence anisotropy of DPH. Cholesterol depletion or enrichment resulted in substantial changes in the motional and orientational properties of DPH, suggesting large structural perturbations in disk membrane phospholipids by cholesterol. Membrane f_v was reduced by cholesterol enrichment, which is consistent with previous studies in model membranes, demonstrating that cholesterol induces increased order in phospholipid acyl chain packing (20, 34).

The retinal chromophore of rhodopsin acts as an excellent reporter of several important conformation changes that occur during formation of the active MII state that binds transducin, the visual G protein. During the activation process, rhodopsin proceeds through a series of photointermediates with distinct conformations, and changes in chromophore conformation and protein-induced electrostatic environment result in distinct absorption spectra for each intermediate (29, 30). In this study the effects of membrane cholesterol on the absorption spectra of three important conformational states of rhodopsin were examined. Dark-adapted rhodopsin is equivalent to an antagonist-bound state, whereas MI is an agonist-bound inactive conformation, and MII is the agonist-bound active conformation that participates in visual signal transduction. The absorption spectra of these three conformational states was unaffected by cholesterol over the entire range of membrane cholesterol concentrations examined as shown in Fig. 4. The lack of variation in the absorption maxima of agonist- or antagonist-bound rhodopsin indicates that no protein conformational changes in the intrahelical retinal-binding domain are induced by cholesterol. Accordingly, specific cholesterol-rhodopsin interactions are unlikely to be involved in the inhibition of rhodopsin conformation changes by cholesterol.

Another line of evidence relative to rhodopsin-cholesterol interactions comes from studies of the effects of membrane cholesterol on acyl chain packing free volume as quantified by f_v and formation of the active MII conformation as quantified by K_{eq}. These quantities are linearly related over the entire range of cholesterol concentrations examined, which was from

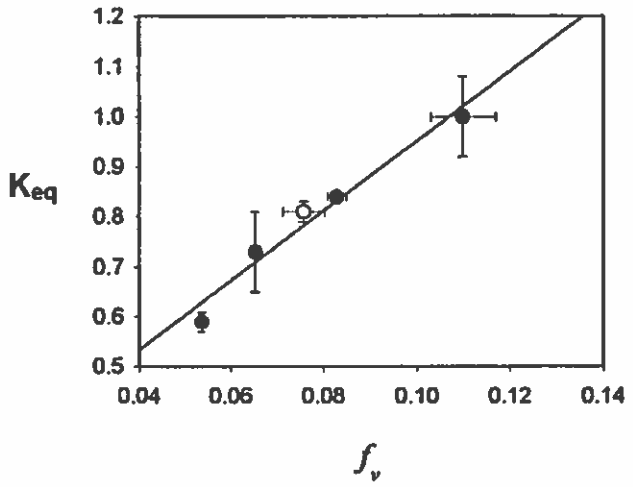

FIG. 6. **Correlation of the MI-MII equilibrium constant, K_{eq}, and the phospholipid acyl chain packing free volume parameter, f_v, from samples varying in cholesterol concentration as described in the legend to Fig. 2 at 37 °C.** The *open circle* is the control disk at 15 mol % cholesterol, which received no MBCD treatment.

4 to 38 mol % (Fig. 6). A linear correlation between K_{eq} and f_v with changes in bilayer cholesterol was observed previously in studies of rhodopsin reconstituted in phospholipid membranes (33). It is significant that the correlation shown in Fig. 6 was obtained for measurements at 37 °C, demonstrating that at physiological temperature cholesterol-induced changes in acyl chain packing and rhodopsin activation are tightly coupled. A reduction of membrane free volume would impose an energy barrier to the MI to MII transition, which is accompanied by a 100 ml/mole volume expansion (35, 36), that would reduce the equilibrium concentration of MII, the active conformation of photoexcited rhodopsin. The effect of reduced free volume in the disk membrane with cholesterol enrichment on rhodopsin conformational flexibility is also demonstrated by the higher thermal stability of rhodopsin in the presence of more ordered acyl chain packing as shown in Fig. 5 and previously by Albert *et al.* (32). Given that cholesterol had no observable structural perturbation on rhodopsin and that K_{eq} and f_v are linearly correlated over the entire range of membrane cholesterol concentration, we conclude that cholesterol inhibits rhodopsin activation via an indirect effect of cholesterol on phospholipid acyl chain packing (*i.e.* by a free volume-mediated mechanism).

A recent study reports that rod outer segment membranes contain detergent-resistant membranes or lipid rafts (37). This term is generally applied to microdomains enriched in cholesterol and sphingomyelin, which are insoluble in mild Triton X-100 at 4 °C (38, 39). The observation relative to ROS disk membranes is unusual in that these membranes contain insignificant amounts of sphingomyelin (13, 14). The results presented in the current study demonstrate that disk membrane cholesterol concentration is inversely correlated with rhodopsin activation as measured by the extent of MII formation. Reducing disk cholesterol from 15 to 4 mol %, which should disrupt or reduce lipid raft formation, actually resulted in higher levels of rhodopsin activation. These results are consistent with recent reports for rhodopsin reconstituted in bilayers formed from phosphatidylcholine and varying levels of cholesterol (26). In these reconstituted systems it is observed that the level (26) and rate (40) of coupling of MII to G protein was inversely correlated with the cholesterol concentration. In the current study a linear correlation was observed between K_{eq} for the MI-MII equilibrium and f_v from 4 to 38 mol % cholesterol at physiological temperature. Here again the results mimic those observed with single component phosphatidylcholine systems with and without cholesterol (8, 33) in which no lipid rafts existed. If increasing cholesterol concentration is accompanied by lateral domain or raft formation in the disk membrane, then this should be manifested as a discontinuity in the cholesterol dependence of the activation of rhodopsin. However, we observed a tight linear correlation of rhodopsin activation with f_v, which is a measure of the bulk or average phospholipid acyl chain packing in the membrane. Therefore, the results of the present study do not show the anticipated evidence for cholesterol-dependent formation of lipid rafts at cholesterol levels well below and above those of the native disk membrane.

Disk phospholipid acyl chains are ~50% DHA, and ~25% of the disk phospholipids contain DHA in both the *sn*-1 and *sn*-2 positions (13). In model membranes formed from di22:6PC, di16:0PC, and cholesterol rhodopsin preferentially partitions into a di22:6PC-rich domain, whereas cholesterol partitions primarily into a domain rich in the saturated phospholipid (31). This observation demonstrates that rhodopsin prefers a liquid-disordered rather than a liquid-ordered phase. Therefore, if lipid rafts exist in disk membranes at physiological conditions and are in the liquid-ordered phase as was reported in other systems then rhodopsin will likely be excluded from these domains. In addition, the evidence from reconstituted systems (26, 40) demonstrates that the presence of cholesterol-induced acyl chain ordering (such as that reported for lipid rafts) would reduce the rate and level of rhodopsin-transducin coupling, thereby diminishing the efficiency of signal transduction. Given the preference of cholesterol for saturated *versus* polyunsaturated acyl chains and the presence of dipolyunsaturated phospholipids in the disk membrane, there is the potential to form cholesterol-enriched and cholesterol-depleted lateral domains in the disk membrane (31). However, given the overall level of polyunsaturated acyl chains in the disk membrane, these domains will likely have very different properties from those found in high sphingomyelin-containing membranes, which might result in a more homogeneous distribution of rhodopsin.

Cholesterol has been found to reduce membrane free volume by ordering phospholipid acyl chain packing. Integral membrane receptors and channels are imbedded in a lipid matrix and need to undergo conformational changes during activation. A simple two-state model described as an inactive state (I) and an activated state (A) illustrates the potential effect of cholesterol on membrane protein function. If the transition from I to A involves a net volume expansion such as the MI to MII transition of photoactivated rhodopsin, a more ordered phospholipid acyl chain packing imposed by cholesterol would inhibit such a transition. Inhibition of membrane protein function would be expected by cholesterol enrichment as is observed in this study. On the other hand, if the transition from I to A involves a net volume reduction, membrane ordering by cholesterol would facilitate such a transition and in turn enhance membrane protein function. The parallel behavior for the cholesterol dependence of rhodopsin activation in the native disk membranes and reconstituted bilayer systems suggests a mechanism of action of cholesterol that involves its effect on phospholipid acyl chain packing. If cholesterol-induced domain formation does occur in disks then their presence may be manifested in the coupling of the protein constituents in the signaling pathway rather than in a direct effect on the conformational changes associated with the activation of rhodopsin. The discussion of the effect of cholesterol on rhodopsin may extend to other membrane proteins as well, including receptors and

channels, which undergo a functional conformational change in a region within the membrane lipid.

REFERENCES

1. Nunez, M. T., and Glass, J. (1982) *Biochemistry* **21**, 4139–4143
2. Fernandez-Ballester, G., Castresana, J., Fernandez, A. M., Arrondo, J. L., Ferragut, J. A., and Gonzales-Ros, J. M. (1994) *Biochemistry* **33**, 4065–4071
3. Gimpl, G., Burger, K., and Fahrenholz, F. (1997) *Biochemistry* **36**, 10959–10974
4. Sooksawate, T., and Simmonds, M. A. (2001) *Neuropharmacology* **40**, 178–184
5. Pang, L., Graziano, M., and Wang, S. (1999) *Biochemistry* **38**, 12003–12011
6. Bastiaanse, E. M., Hold, K. M., and Van der Larse, A. (1997) *Cardiovasc. Res.* **33**, 272–283
7. Mitchell, D. C., Straume, M., and Litman, B. J. (1992) *Biochemistry* **31**, 662–670
8. Litman, B. J., and Mitchell, D. C. (1996) *Lipids* **31**, (suppl.) S193–S197
9. Litman, B. J., and Mitchell, D. C. (1996) in *Biomembranes* (Lee, A., ed) pp. 1–32, JAI Press, Greenwich, CT
10. Straume, M., Mitchell, D. C., Miller, J. L., and Litman, B. J. (1990) *Biochemistry* **29**, 9135–9142
11. Boesze-Battaglia, K., Hennessey, T., and Albert, A. D. (1989) *J. Biol. Chem.* **264**, 8151–8155
12. Boesze-Battaglia, K., and Albert, A. D. (1990) *J. Biol. Chem.* **265**, 20727–20730
13. Stinson, A. M., Wiegand, R. D., and Anderson, R. E. (1991) *Exp. Eye Res.* **52**, 213–218
14. Yuan, C., Chen, H., Anderson, R. E., Kuwata, O., and Ebrey, T. G. (1998) *Comp. Biochem. Physiol. B Biochem. Mol. Biol.* **120**, 785–789
15. Smith, H. G. J., and Litman, B. J. (1982) *Methods Enzymol.* **81**, 57–61
16. Papermaster, D. S., and Dreyer, W. J. (1974) *Biochemistry* **13**, 2438–2444
17. Palczewski, K., Kumasaka, T., Hori, T., Behnke, C. A., Motoshima, H., Fox, B. A., Trong, I. L., Teller, D. C., Okada, T., Stenkamp, R. E., Yamamoto, M., and Miyano, M. (2000) *Science* **289**, 739–745
18. Hargrave, P. A. (2001) *Investig. Ophthalmol. Vis. Sci.* **42**, 3–9
19. Straume, M., and Litman, B. J. (1987) *Biochemistry* **26**, 5113–5120
20. Mitchell, D. C., and Litman, B. J. (1998) *Biophys. J.* **75**, 896–908
21. Allain, C. C., Poon, L. S., Chan, C. S., Richmond, W., and Fu, P. C. (1974) *Clin. Chem.* **20**, 470–475
22. Miller, J. L., Fox, D. A., and Litman, B. J. (1986) *Biochemistry* **25**, 4983–4988
23. Bartlett, G. R. (1959) *J. Biol. Chem.* **234**, 587–596
24. Jackson, M. L., and Litman, B. J. (1985) *Biochim. Biophys. Acta* **812**, 369–376
25. Lowry, O. H., Rosebrough, N. J., Farr, A. L., and Randall, R. J. (1951) *J. Biol. Chem.* **193**, 265–272
26. Niu, S. L., Mitchell, D. C., and Litman, B. J. (2001) *J. Biol. Chem.* **276**, 42807–42811
27. Mitchell, D. C., and Litman, B. J. (1998) *Biophys. J.* **74**, 879–891
28. Johnson, M. L., and Faunt, L. M. (1992) *Methods Enzymol.* **210:1–37**, 1–37
29. Lewis, J. W., and Kliger, D. S. (1992) *J. Bioenerg. Biomembr.* **24**, 201–210
30. Yoshizawa, T., Shichida, Y., and Matuoka, S. (1984) *Vision Res.* **24**, 1455–1463
31. Polozova, A., and Litman, B. J. (2000) *Biophys. J.* **79**, 2632–2643
32. Albert, A. D., Boesze-Battaglia, K., Paw, Z., Watts, A., and Epand, R. M. (1996) *Biochim. Biophys. Acta* **1297**, 77–82
33. Mitchell, D. C., Straume, M., Miller, J. L., and Litman, B. J. (1990) *Biochemistry* **29**, 9143–9149
34. Straume, M., and Litman, B. J. (1987) *Biochemistry* **26**, 5121–5126
35. Attwood, P. V., and Gutfreund, H. (1980) *FEBS Lett.* **119**, 323–326
36. Lamola, A. A., Yamane, T., and Zipp, A. (1974) *Biochemistry* **13**, 738–745
37. Seno, K., Kishimoto, M., Abe, M., Higuchi, Y., Mieda, M., Owada, Y., Yoshiyama, W., Liu, H., and Hayashi, F. (2001) *J. Biol. Chem.* **276**, 20813–20816
38. London, E., and Brown, D. A. (2000) *Biochim. Biophys. Acta* **1508**, 182–195
39. Simons, K., and Ikonen, E. (1997) *Nature* **387**, 569–572
40. Mitchell, D. C., Niu, S. L., and Litman, B. J. (2001) *J. Biol. Chem.* **276**, 42801–42806